

Subglass and Glass Transitions of Poly(di-*n*-alkylitaconate)s with Various Side-Chain Lengths: Solid-State NMR Investigation

A.-C. Genix*,† and F. Lauprêtre*

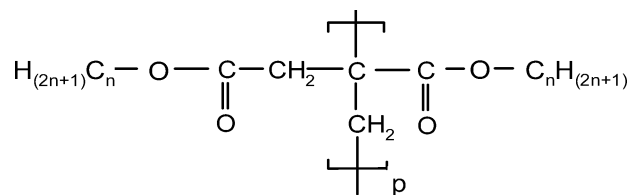
Laboratoire de Recherche sur les Polymères, UMR 7581 CNRS, 2 à 8 rue Henri Dunant, 94320 Thiais, France

Received March 31, 2006; Revised Manuscript Received July 7, 2006

ABSTRACT: Variable-temperature high-resolution solid-state ^{13}C NMR experiments were performed on poly-(di-*n*-alkylitaconate)s in bulk. Temperature-dependent line broadenings resulting from either motional modulation of the ^{13}C – ^1H dipolar coupling or motional modulation of the chemical shift anisotropy were observed for each carbon atom of the polymer main chain and side chains. Similarly, independent determinations of the ^{13}C – ^1H dipolar couplings and ^{13}C chemical shift anisotropies demonstrated the existence of local motions in solid poly-(di-*n*-alkylitaconate)s. All of these measurements led to a direct identification of the moving units that are involved in the various relaxations, which were previously investigated by using dielectric relaxation experiments.

1. Introduction

Poly(di-*n*-alkylitaconate)s (PDAI) are known to exhibit several relaxations related to the development of specific motional processes in the solid state. Their chemical formula is:



where *n* is the number of carbons in the alkyl side chains. The different subglass and glass relaxation processes in PDAI's have been studied for a long time mainly by differential scanning calorimetry (DSC),^{1,2} dynamic mechanical analysis (DMA),^{3–6} dielectric spectroscopy,^{7–9} and recently, by solution NMR and molecular modeling,¹⁰ which led to a deeper understanding of the relative role of intramolecular constraints and intermolecular interactions in the solid-state organization and properties of these polymers. The dielectric relaxation measurements⁹ were performed on a series of poly(di-*n*-alkylitaconate)s with various side-chain lengths. This work allowed clarification of the complex relaxational behavior in these polymers and definition of the location of the secondary relaxations in the temperature and frequency domains. The comparison of the results obtained by increasing the length of the side groups permitted an assignment of the γ , β_{fast} , and β_{slow} secondary relaxations to motions of the alkyl side chains, of the ester groups located after the CH_2 unit and of the ester groups directly attached to the main chain, respectively. In poly(di-*n*-alkylitaconate)s with six carbon atoms at least in the alkyl part, the existence of an additional low-temperature glass transition, α^L , was clearly established. The α^L process replaces the β_{fast} process observed in the lower derivatives. It is located in quite the same

temperature and frequency ranges and exhibits a non-Arrhenius behavior. It is likely related to cooperative motions of the alkyl side chains and ester group next to the CH_2 spacer unit.

The aim of the present study is to get a more detailed interpretation of the dielectric relaxation experiments⁹ mentioned above by achieving a precise identification of the molecular motions that are responsible for each relaxation in the solid state. Among the various techniques that can be used to examine the local mobility in polymers, high-resolution solid-state ^{13}C NMR is a very powerful tool because it is a selective method that permits following the motional behavior of each carbon of the repeat unit independently. Moreover, many different NMR parameters may be used to study molecular motions. Experiments described in the present paper are mainly based on ^{13}C line-width measurements over a wide temperature range and independent determinations of the ^{13}C – ^1H dipolar couplings and ^{13}C chemical shift anisotropies. Results thus obtained are discussed in close relation with the previous dielectric data,⁹ and the molecular origin of the different processes is carefully investigated.

2. Experimental Section

Dialkyl itaconic esters with side-chain lengths with *n* = 1, *n* = 3, and *n* = 6 were prepared by esterification of itaconic acid using the appropriate alcohol. Bulk polymerizations using α,α' -azobisisobutyronitrile as an initiator were carried out under nitrogen and polymers were isolated by precipitation into methanol.³ Code names and molecular weights, M_n and M_w , as determined from size exclusion chromatography in THF for the three polymers, are listed in Table 1. Glass-transition temperatures, T_g , were derived from the onset of the baseline shift observed in heat capacity measurements by using a TA instrument differential scanning calorimeter 2010 operating at 20 K min^{-1} . T_g values thus obtained are given in Table 1. Note that, for PDHI, there is an indication of an additional low-temperature inflection in the variation of the heat capacity as a function of temperature in agreement with results reported by Cowie et al.⁶ for the higher PDAI derivatives.

High-resolution solid-state ^{13}C NMR spectra were recorded at 75.47 MHz using a Bruker Avance 300 WB spectrometer. A variable temperature 4 mm magic angle spinning (MAS) probe head was used. Samples were packed in zirconium dioxide rotors closed with boron nitride caps and spun at 6.5 kHz unless otherwise specified. The inner spinner volume was approximately 0.1 cm^3 . All spectra were obtained by cross-polarization (CP) from the spin-

* Corresponding Authors. E-mail: laupretre@glvt-cnrs.fr (F.L.); swxgegec@sw.ehu.es (A.-C.G.). Telephone: +33 1 49 78 12 86 (F.L.). Fax: +33 1 49 78 12 08 (F.L.).

† Present address: Donostia International Center, Paseo Manuel de Lardizabal 4, 20018 San Sebastián, Spain.

Table 1. Characterization of the Samples

code	<i>n</i>	name	$10^{-4} M_n$ (g mol ⁻¹)	$10^{-4} M_w$ (g mol ⁻¹)	T_g (DSC) (°C)
PDMI	1	poly(dimethylitaconate)	7.4	9.4	92
PDPI	3	poly(di- <i>n</i> -propylitaconate)	18.6	48.2	20
PDHI	6	poly(di- <i>n</i> -hexylitaconate)	8.7	19.1	-38

locked protons, followed by high-power proton dipolar decoupling (DD). The matched spin-locked cross-polarization transfers were carried out with ¹H magnetic field strength of 62.5 kHz, corresponding to a $\pi/2$ pulse duration of 4 μ s. The Hartmann–Hahn condition was matched using glycine with a very short contact time of 20 μ s. The proton decoupling field strength was 80 kHz. Chemical shift calibrations were performed using the glycine carbonyl carbon resonance at 176 ppm. Contact time and repetition time were 1 ms and 2 s, respectively. About 2000 scans were needed to obtain a suitable signal-to-noise ratio. Spectra were recorded in the temperature range from -110 to 40 °C. The temperature was controlled with a Bruker BVT 3000 to an accuracy of ± 0.1 K. It was calibrated by using the temperature-dependent chemical shift of Pb(NO₃)₂ over the range from -130 to +150 °C.¹¹ For experiments performed below room temperature, a low-temperature kit using liquid nitrogen evaporation was connected to the probe head.

In the cross-polarization experiments, molecular mobility was investigated by examining the effect that different contact times have on the development of magnetization of protonated carbons. The $t_{1/2}$ cross-polarization time is defined as the contact time necessary to get half of the maximum value of the magnetization (M_{\max}) that can be achieved by cross-polarization. M_{\max} was derived by fitting the exponential $T_{1\rho}(^1\text{H})$ decay of the ¹³C magnetization observed at long contact times and extrapolating it to zero time.

The principal values of the chemical shift anisotropy tensors of the carbonyl carbons were derived from the relative intensities of the spinning sidebands recorded for slowly spinning samples by utilizing Herzfeld and Berger calculations.¹²

3. Theoretical Background

Line-broadening mechanisms in glassy polymers have already been reviewed.¹³ Some of them, the static ones, i.e., bulk susceptibility of the sample, chemical shift dispersions due to packing effects, bond distortions, and conformational inequivalence, induce only a relatively small effect, $(\pi T_{2\text{res}})^{-1}$, on the order of 2–6 ppm. More important are the line broadenings arising from relaxation mechanisms such as motional modulation of the dipolar carbon–proton coupling,¹⁴ $(\pi T_{2m})^{-1}$, and motional modulation of the chemical shift anisotropy (CSA),¹⁵ $(\pi T_{2\sigma})^{-1}$. Therefore, in the general case, the observed line width at half-height may be written as:

$$\Delta\nu_{1/2} = \frac{1}{\pi T_{2\text{res}}} + \frac{1}{\pi T_{2m}} + \frac{1}{\pi T_{2\sigma}} = \frac{1}{\pi T_2} \quad (1)$$

For carbons having a strong dipolar carbon–proton coupling (protonated carbons) under suitable conditions of magic-angle setting and proton-decoupling irradiation, the main cause of motional line broadening is the modulation of the dipolar ¹³C–¹H coupling. This mechanism gives a maximum line broadening when the rate of molecular motion is equal to the proton-decoupling radio frequency field strength, $\omega_{1\text{H}}$, expressed in angular frequency units. For motions with correlation times in the range from 10^{-5} to 10^{-7} s, the corresponding line broadening may be much larger than the one due to the static effects. Under the conditions where the proton irradiation is applied exactly on resonance and where the sample spinning rate is much smaller than the proton-decoupling field strength, the transverse relaxation time resulting from this mechanism and contributing

an amount of $(\pi T_{2m})^{-1}$ to the line width is:

$$\frac{1}{T_{2m}} = \frac{1}{2} \langle \Delta M_{\text{CH}}^{(2)} \rangle J(\omega_{1\text{H}}) \quad (2)$$

where $\langle \Delta M_{\text{CH}}^{(2)} \rangle$ is the part of the truncated carbon–proton second moment that is modulated by the motion, and $J(\omega_{1\text{H}})$ is the spectral density associated with the fluctuations of the dipolar interaction at the frequency $\omega_{1\text{H}}$. In the following, the motion of the CH₂ and CH₃ units will be described in terms of stochastic jumps characterized by a correlation time, τ_c , of the internuclear C–H vector around their local rotation axis.¹⁶ By assuming a fixed rotation axis for the unit under consideration, the spectral density of motion is written as:

$$J(\omega) = K \left[B \frac{2\tau_c}{1 + \omega^2 \tau_c^2} + C \frac{2(\tau_c/4)}{1 + \omega^2 (\tau_c/4)^2} \right] \quad (3)$$

where $B = 3/4 \sin^2(2\Delta)$, $C = 3/4 \sin^4\Delta$, Δ is the angle between the internuclear vector and the rotation axis, and K is a constant.

For carbons having a high chemical shift anisotropy (unsaturated carbons), the motional modulation of the chemical shift anisotropy induces a line broadening, $(\pi T_{2\sigma})^{-1}$, which is maximum when the rate of molecular motion is equal to the rotor spinning speed, ω_{MAS} . In the limiting case of the weak collision regime, i.e., when the spinning speed is much larger than the chemical shift anisotropy expressed in Hz, the transverse relaxation time is written as¹³

$$\frac{1}{T_{2\sigma}} = (\gamma B_0 \Delta \sigma)^2 J(\omega_{\text{MAS}}) \quad (4)$$

where $\Delta \sigma$ is a root-mean-square instantaneous change in chemical shift produced by change in spatial orientation. In the following, the motion of the carbonyl carbons will be described in terms of random jumps between two equilibrium positions by using the spectral density¹⁶

$$J(\omega) = KB \frac{2\tau_c}{1 + \omega^2 \tau_c^2} \quad (5)$$

with the same definition for the B and K coefficients as in eq 3. The calculation of τ_c was performed within the assumption of the weak collision model, i.e., in the temperature range above the temperature T_{min} , where the minimum of T_2 is observed.

In the presence of local motions, the motional averaging of the ¹³C–¹H dipolar coupling can also be investigated by using $t_{1/2}$ measurements that are based on the rises of the ¹³C magnetization in cross-polarization experiments with very short contact times.¹⁷ Values of $t_{1/2}$ as short as 17 μ s for a CH₂ group or 20 μ s for a CH group are indicative of rigid-lattice behavior. Longer values are evidence for a reduction in dipolar coupling by motional processes with frequency of the order of or higher than 10^5 Hz.¹⁷

4. Results

4.1. Poly(dimethylitaconate). Poly(dimethylitaconate) is an interesting sample to begin with, as its side chain is the shortest in the PDAI series. MAS/CP/DD ¹³C NMR spectra of solid PDMI as a function of temperature are plotted in Figure 1. They consist of several lines that were identified on the basis of previous results.^{18,19} The line assignment is summarized in Figure 1. As shown on this figure, the ¹³C line widths of each carbon of the repeat unit are strongly modified on varying

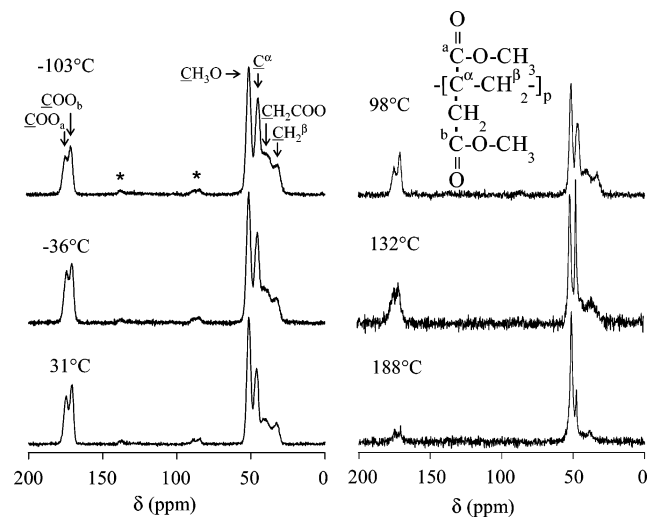


Figure 1. MAS/CP/DD ^{13}C NMR (75 MHz) spectra of solid poly(di-methylitaconate) at different temperatures. The spectral assignments are shown on the ^{13}C NMR spectrum at -103°C (asterisks indicate the spinning sidebands). Inset, chemical formula of PDMI.

temperature. In the following part, the temperature dependence of the different lines will be described. We will start from the end of the side chain (methyl group) and then move step by step toward the main chain.

OCH₃. At the lowest temperature investigated (-103°C) the line due to the methyl carbon is relatively broad, in sharp contrast with the narrow line that is observed at high temperature. At each temperature, the transverse relaxation time, T_2 , was deduced from the line width at half-height by using eq 1, and the data thus obtained are reported in Figure 2a. The T_2 curve shows indication of a relative minimum in the temperature range between -10 and 10°C , which suggests that the motional modulation of the dipolar carbon–proton coupling is maximum over this range. Therefore, in this temperature range between -10 and 10°C , the methyl groups of PDMI are involved in molecular motions at a frequency close to the proton-decoupling field strength expressed in frequency units (ca. 83 kHz). For higher temperatures and up to 120°C , the rate of molecular motion of these units increases and a line-narrowing follows on the ^{13}C NMR spectra as the ^{13}C – ^1H dipolar interaction is motionally averaged. A second minimum is then observed at 154°C that can be associated with a second motional process of the OCH₃ units at frequencies of the order of 83 kHz. It must also be noticed that, at very low temperatures between -103 and -25°C , a slight decrease of the T_2 values occurs. It corresponds to a line broadening of 10 Hz and can be, therefore, attributed to inhomogeneities in the static magnetic field (we checked that a glycine sample displays a similar line broadening in the low-temperature range). As a consequence of this experimental effect, the increase of T_2 due to molecular motions below the first minimum for OCH₃ is hidden.

COO. The repeat unit of PDAI's contains two carbonyl groups that are denoted as COO_a and COO_b (see formula given in Figure 1). The resonance lines due to these carbons are located at 171.1 and 174.9 ppm, respectively. Whereas, at low temperature, they are reasonably well-resolved, the lines are so broadened above 100°C that the resolution has completely disappeared (Figure 1). As mentioned above, the line broadening for such unsaturated carbons is dominated by motional modulation of the chemical shift anisotropy. To determine the transverse relaxation times, the broadened COO_a and COO_b lines were decomposed using Lorentzian functions (see inset in Figure 2b)

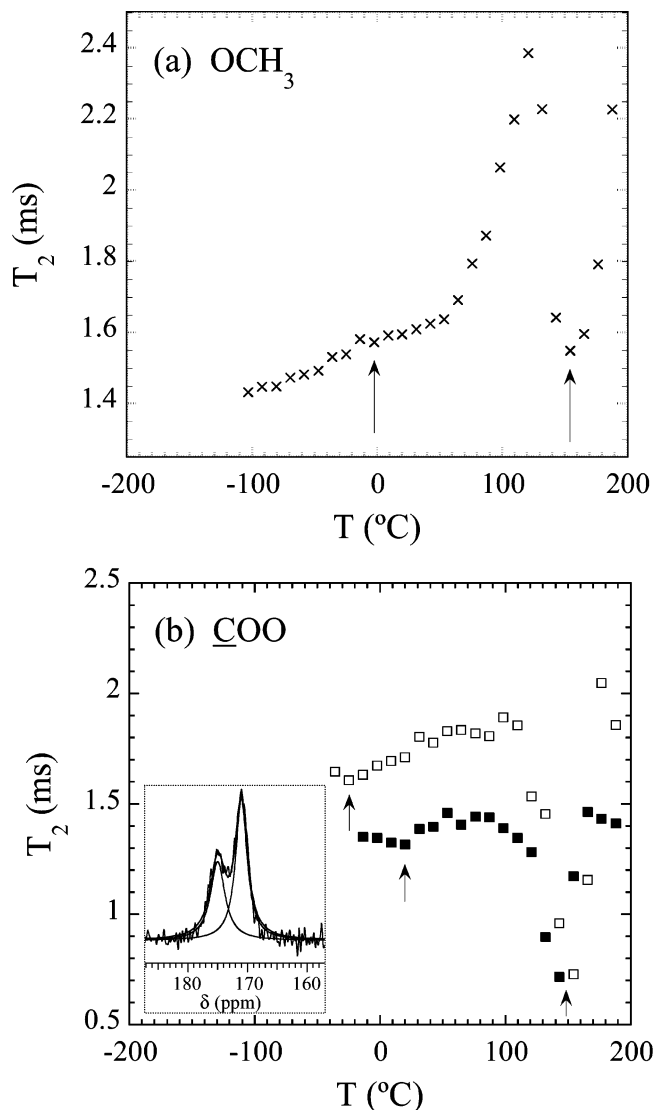


Figure 2. Transverse relaxation times, T_2 , of (a) the OCH₃ carbon and (b) the COO_a (■) and COO_b (□) carbonyl groups in poly(di-methylitaconate) as a function of temperature. Arrows indicate the position of the different T_2 minima. Inset in (b) displays the line shape decomposition for the carbonyl lines at 87°C .

centered on the chemical shift determined from the room-temperature ^{13}C NMR spectrum. The temperature dependence of T_2 for both carbonyl groups is shown in Figure 2b. They exhibit two minima. The first minimum, with relatively weak amplitude, occurs around -25 and 21°C for the COO_b and COO_a carbons, respectively, implying that, at these temperatures, the frequency of molecular motions is of the order of the spinning speed (ca. 6.5 kHz). It can be seen in Figure 1 that the peaks for the carbonyls are very well-defined in this temperature range, and a realistic error for the T_2 values would be of the order of 2–3% in this range. The second minimum, of larger amplitude, is located around 150°C for both carbons. This result indicates that, above 150°C , all the carbonyl units are involved in molecular motions with frequencies superior or equal to 6.5 kHz. It can also be noticed that the T_2 decrease around the high-temperature minimum is more important for COO_b than for COO_a. As the transverse relaxation time is inversely proportional to the part of the second moment that is modulated by the motion, it can be concluded that the motional contribution to the line width is larger for COO_b. As previously suggested,⁷ the presence of a CH₂ spacer unit between the main chain and

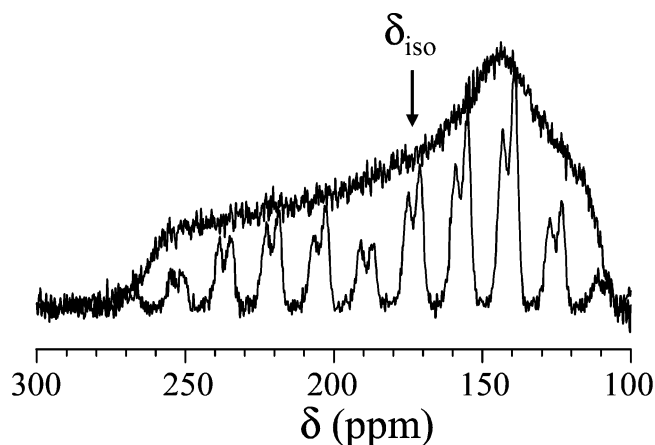


Figure 3. Static CP/DD and MAS/CP/DD ^{13}C NMR spectra of the PDMI COO carbons obtained with a 1.2 kHz spinning speed at room temperature.

Table 2. Principal Components of the PDMI COO Chemical Shift Tensors at Low Temperature

	T (°C)	σ_{11}	σ_{22}	σ_{33}
COO_b	-98	-91	25	66
$\text{CH}_3\text{COOCH}_3$ (Mehring ²¹)	-140	-85	22	62
COO_a	-98	-89	26	62
HCOOCH_3 (Mehring ²¹)	-186	-88	29	58

the carbonyl group, tends to increase the mobility of the carbonyl group.

The line broadening observed around 150 °C for the OCH_3 , COO_a , and COO_b units leads to a spectrum collapse, characteristic of amorphous polymers at the glass-transition temperature.²⁰ Above T_g , the ^{13}C – ^1H dipolar coupling and the chemical shift anisotropy are strongly averaged by fast motions of the polymer and the line widths decrease. Note also that, because of the local motions of the chain, the cross polarization at high temperature is less efficient, leading to a sensitivity loss over the full ^{13}C NMR spectrum (Figure 1).

Turning now to the independent determination of the chemical shift anisotropy, the ^{13}C NMR spectrum of the COO_a and COO_b carbons, recorded at 25 °C with a spinning speed of 1.2 kHz, is given in Figure 3 as an example. The principal values of the chemical shift tensors, determined from the spinning sideband intensities at very low temperature by using Herzfeld and Berger calculations,¹² are summarized in Table 2. They are in good agreement with values measured by Mehring²¹ for the COO group of methyl acetate. As shown in Figure 4a, on increasing temperature, the chemical shift anisotropy of the COO_a and COO_b carbons decreases, indicating that the chemical shift tensors are partly averaged by local motions. The oscillation amplitude of the carbonyl groups, calculated²² from data reported in Figure 4a, is displayed in Figure 4b as a function of temperature. We can note that, at the temperatures for which the T_2 minima are observed at low temperature (arrows in Figure 4b), the oscillation amplitude is of the order of ± 20 °C. This result supports the existence of the low-temperature T_2 minima observed in Figure 2b. In this context, the low-temperature relaxation of each carbonyl group can be described in terms of oscillations around the C–C_{ester} axis, which links the side chain to the main chain. At high temperature, the motional behavior of the carbonyl groups was investigated in more detail by using the dynamic order parameter, $\langle P_2 \rangle$, defined by Kulik et al.²³ as

$$\langle P_2 \rangle = \frac{\sigma_{33}(T) - \sigma_{\text{iso}}}{\sigma_{33}(0) - \sigma_{\text{iso}}} \quad (6)$$

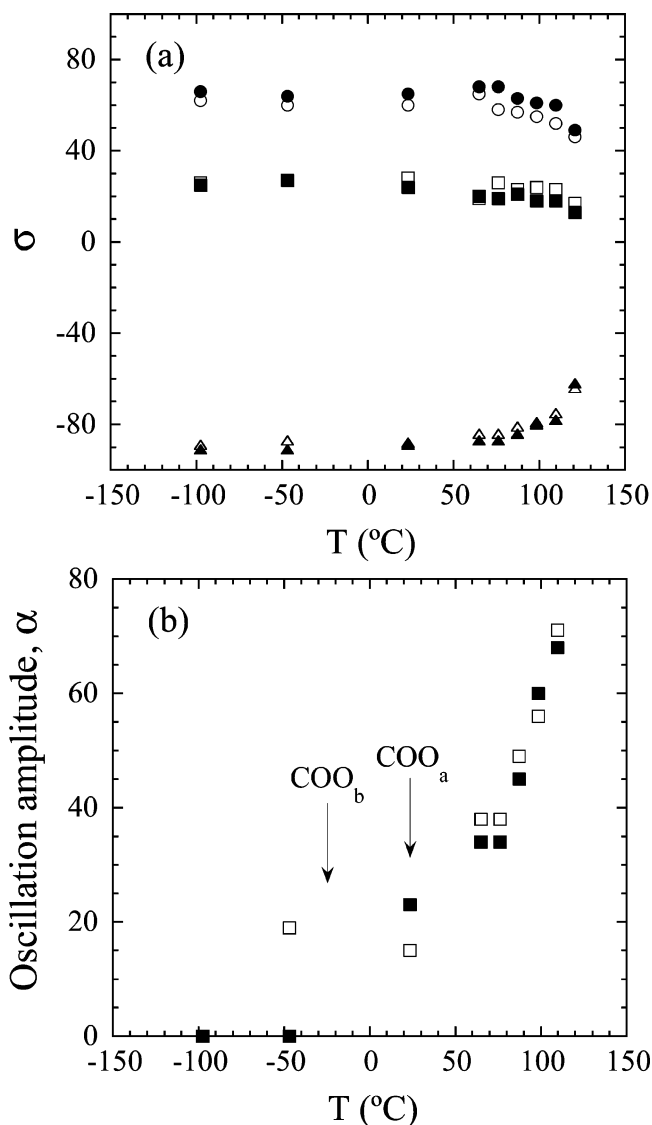


Figure 4. (a) Principal values of the chemical shift tensor derived from standard procedure:¹² σ_{11} (\blacktriangle , \triangle), σ_{22} (\blacksquare , \square), and σ_{33} (\bullet , \circ): empty and filled symbols correspond to COO_a and COO_b units, respectively. (b) Temperature dependence of the oscillation amplitude, α , of the PDMI COO_a (\blacksquare) and COO_b (\square) units.

where $\sigma_{33}(T)$ corresponds to the most upfield tensor principal value at a given temperature and $\sigma_{33}(0)$ is the rigid lattice value, which has been taken here as the value determined at the lowest temperature investigated. As can be observed in Figure 5, the dynamic order parameter is equal to 1 within experimental error for temperatures lower than 70 °C. It decreases for temperatures higher than 70 °C, i.e., at temperatures higher than the temperature range of the low-temperature relaxation of the COO_b and COO_a carbons. $\langle P_2 \rangle$ is equal to 0.75 at 121 °C, which is close to the α relaxation temperature at the frequency of the present NMR experiment. This result shows that, in agreement with results reported by Bordes²⁴ on poly(methyl methacrylate) (PMMA), large-amplitude motions of the carbonyl groups require a significant reorientation of the local main-chain axis that can only occur in the vicinity of the glass transition.

Main Chain. Another interesting feature, observed on increasing temperature, is the chemical shift variation of the lines associated to the quaternary carbon (C^α) and methylene group (CH_2^β) of the main chain, and to the methylene spacer group (CH_2COO). Figure 6a displays the ^{13}C NMR spectra in the chemical shift region of interest at different temperatures in the

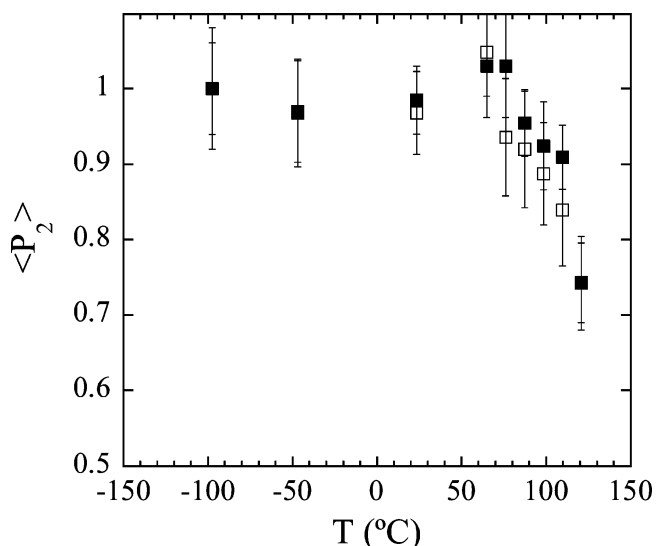


Figure 5. Dynamic order parameter, $\langle P_2 \rangle$, calculated from the chemical shift anisotropy of the COO_a (■) and COO_b (□) carbons in PDMI as a function of temperature

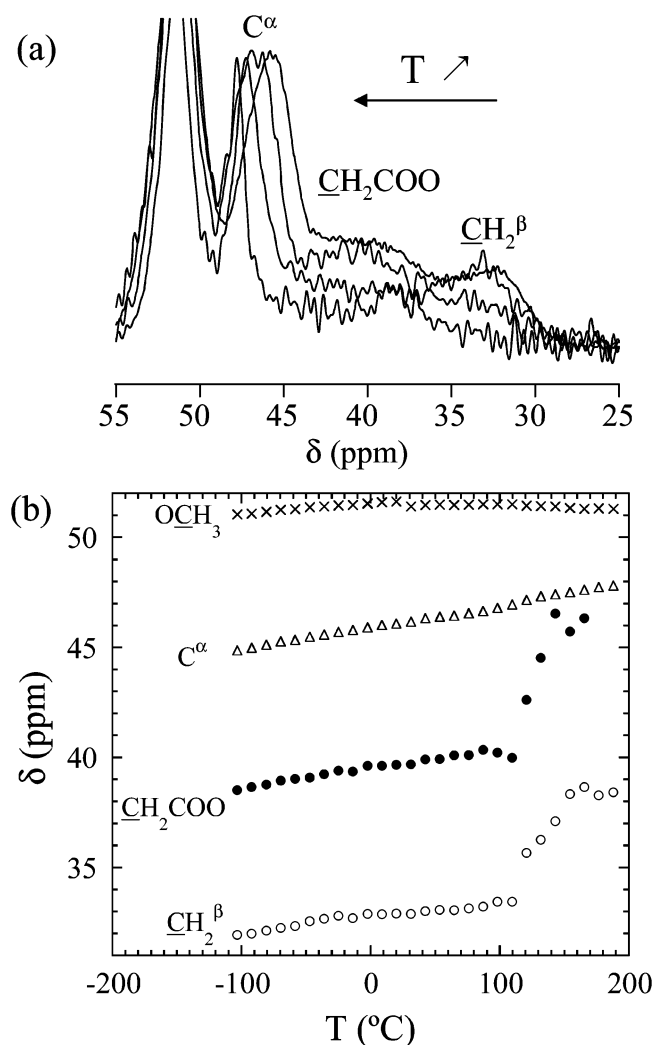


Figure 6. (a) MAS/CP/DD ^{13}C NMR (75 MHz) spectra of solid poly(dimethylitaconate) at 25, 100, 120, and 190 °C (from right to left) in the region of the C^α , CH_2^β , and CH_2COO carbons. (b) Chemical shift variation of the corresponding carbons as a function of temperature: data obtained for the OCH_3 carbon are added for comparison.

range from 25 to 190 °C. As illustrated in Figure 6b, a 2 ppm variation of the C^α chemical shift is observed over the whole

temperature range investigated, with a 1 ppm increase between 100 and 120 °C. The chemical shifts of the CH_2^β and CH_2COO methylene carbons are determined by fitting each resonance peak by a Lorentzian function; they exhibit a strong increase of about 5 ppm between 110 and 150 °C. Note that, for the CH_2COO methylene carbon, the large shift of the resonance peak toward lower field leads to the merging of this line with the C^α line above 165 °C. For comparison, the temperature dependence of the chemical shift of the methyl carbon is also shown in Figure 6b. The chemical shift variations observed for the three main-chain carbons are clearly indicative of conformational changes of the main-chain or adjacent side-chain bonds with a motional frequency that may be estimated to 75 Hz for C^α and to 375 Hz for the CH_2^β and CH_2COO units, based on equations describing site exchange in NMR.²⁵ Moreover, the appearance of the onset of motion at the same temperature for the CH_2^β and CH_2COO methylene carbons strongly suggests the existence of correlated motions for these two units in the temperature range of interest. A classical interpretation of the ^{13}C chemical shift variation as a function of temperature is provided by the conformationally sensitive γ -gauche substituent effect.²⁶ It has been demonstrated that the orientation of the central C–C bond between a given carbon and its γ substituent strongly affects the chemical shift of the observed carbon. For example, a gauche conformation may lead to a shift of the ^{13}C resonance peak toward a higher field up to 5 ppm. Unfortunately, in the case of PDMI, the quaternary carbon holds no less than eight γ substituents. The CH_2^β and CH_2COO units have six and three γ substituents, respectively. Therefore, the detailed interpretation of data reported in Figure 6 in terms of conformations and conformational changes is not an easy task. A similar difficulty was previously reported for PMMA,²⁷ whose chemical structure is close to the PDMI structure. By using ab initio calculations, Born and Spiess²⁷ did not get a good agreement between PMMA experimental ^{13}C chemical shifts and calculated data. Such a discrepancy was explained in terms of strong sterical constraints that determine the values of the bond and dihedral angles of the PMMA main chain and, therefore, strongly affect the ^{13}C chemical shifts in a way that dominates the classical γ -gauche effect.

In addition to the line-width investigation, the temperature dependence of $t_{1/2}$ was determined for the two methylene units in the main chain. The $t_{1/2}$ values obtained for the CH_2^β and CH_2COO carbons are shown in Figure 7a. Between room temperature and 165 °C, they are equal to 17 μs , which is the rigid-lattice value for CH_2 groups. This result indicates that the CH_2 carbons do not undergo local motions at a frequency equal to or higher than 10^5 Hz in this temperature range. Above 165 °C for CH_2^β , there is a clear reduction of the strength of the dipolar coupling, indicating the existence of motional processes of the main chains in the 10^5 Hz region. At 188 °C, the values obtained for the $t_{1/2}/t_{1/2\text{-rigid}}$ ratio can be interpreted in terms of correlated conformational jumps²⁸ within the main chains.

4.2. Poly(di-*n*-propylitaconate). MAS/CP/DD ^{13}C NMR spectra of PDPI recorded at various temperatures are plotted in Figure 8, which also includes the spectral assignment and the chemical formula of PDPI. As observed for PDMI, on varying temperature, the spectra exhibit strong variations of the width at mid-height and of the chemical shift of the main-chain carbons.

As shown in Figure 8, the resonance lines associated with the CH_3 and CH_2 carbons at low temperature are much broader than the lines recorded at 143 °C, and between these two

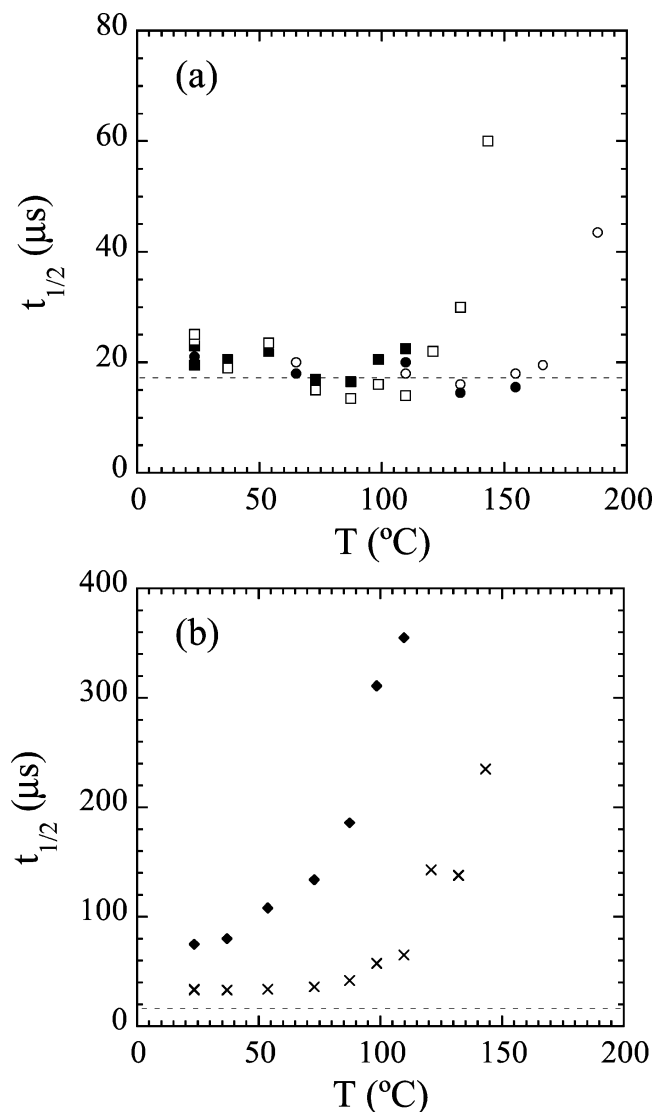


Figure 7. Temperature dependence of $t_{1/2}$ measured for (a) the CH_2^{β} (\circ , \square) and CH_2COO (\bullet , \blacksquare) carbons in PDMI and PDPI, respectively, and (b) the OCH_2 (\times) and CH_2 (\blacklozenge) side-chain carbons in PDPI. The dotted line indicates the value of $t_{1/2}$ in the absence of motions.

temperatures, intermediate characteristics are observed. The variations of T_2 as a function of temperature are plotted in Figure 9a for these two carbons. They exhibit two minima around -114 $^{\circ}\text{C}$ and in the temperature range from 100 to 120 $^{\circ}\text{C}$, respectively. Properly speaking, we are not observing a minimum at -114 $^{\circ}\text{C}$, as this is just the lowest temperature for which we have data and the minimum may be located at even lower temperatures. However, it has to be emphasized that we are going toward a minimum on decreasing temperature, i.e., we are observing the development of a molecular motion for these units. Here, and in the following, we will assume that the position of the minimum is close to -114 $^{\circ}\text{C}$ (we will see later that this hypothesis is corroborated by our previous dielectric study⁹). As discussed above, the modulation of the carbon–proton dipolar coupling by the motion is maximum where T_2 is minimum, and at the corresponding temperatures (-114 $^{\circ}\text{C}$ and around 110 $^{\circ}\text{C}$), the motional frequency is of the order of 83 kHz. It must also be noticed that, in both cases, the amplitude of the minimum at low temperature is significantly higher than the broadening due to inhomogeneities in the static magnetic field.

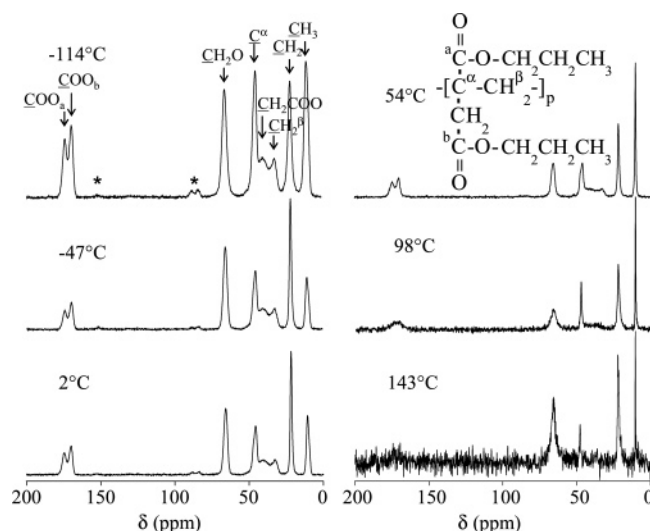


Figure 8. MAS/CP/DD ^{13}C NMR (75 MHz) spectra of solid poly(di-*n*-propylitaconate) at different temperatures. The spectral assignments are shown on the ^{13}C NMR spectrum at -114 $^{\circ}\text{C}$ (asterisks indicate the spinning sidebands). Inset: chemical formula of PDPI.

The temperature dependence of T_2 for the OCH_2 carbon is plotted in Figure 9b. Two minima are observed in the T_2 curve: a first minimum with low amplitude around -114 $^{\circ}\text{C}$ and a second minimum with stronger amplitude at 121 $^{\circ}\text{C}$. Each minimum is associated with motions whose frequencies are of the order of 83 kHz. $t_{1/2}$ values for the OCH_2 and CH_2 units of the PDPI side chains are plotted in Figure 7b as a function of temperature. For both carbons, the room-temperature $t_{1/2}$ is higher than the rigid-lattice value and attests to a significant mobility of the side chains at this temperature. This result is in good qualitative agreement with the present line-width measurements, which show the existence of a T_2 minimum around -114 $^{\circ}\text{C}$ for these carbons. Beyond room temperature, the movements develop progressively as shown by the $t_{1/2}$ increase, and this increase becomes faster at temperatures higher than 100 $^{\circ}\text{C}$.

As can be seen in Figure 8, the lines for the COO_a and COO_b carbons are poorly resolved. In the high-temperature range, the NMR spectra are very noisy and, therefore, data above 120 $^{\circ}\text{C}$ were not used in the following. Below 120 $^{\circ}\text{C}$, the NMR spectra were decomposed using two Lorentzian functions in order to obtain the individual relaxation times at each temperature. The T_2 curves in Figure 9c show a minimum with strong amplitude for the COO_a and COO_b carbons around 98 and 110 $^{\circ}\text{C}$, respectively. Although the minima in the high temperature side are defined by only one or two points, the difference in the amplitude between these points is high enough to be confident about the existence of the minima. As the precise position of the peaks is determined from the room-temperature spectrum, the error bars for T_2 take reasonable values ($\approx 15\%$), even in the 110–120 $^{\circ}\text{C}$ temperature range where the sensitivity of the spectra tends to decrease. Close to the minimum, the decrease of T_2 is more significant for the COO_b carbon. As for PDMI, it indicates that the motional amplitude is larger for the carbonyl group, which is separated from the main chain by a CH_2 unit. For COO_b , a second ill-defined minimum can be detected around -50 $^{\circ}\text{C}$. In the temperature range from -50 to 10 $^{\circ}\text{C}$, the width of the line associated with this carbon increases by 12 Hz. No indication of a second minimum can be seen for the COO_a carbon for which the T_2 values in this temperature range are nearly constant. It must be observed that the decrease of the T_2 values, common to both COO carbons below -70 $^{\circ}\text{C}$, corre-

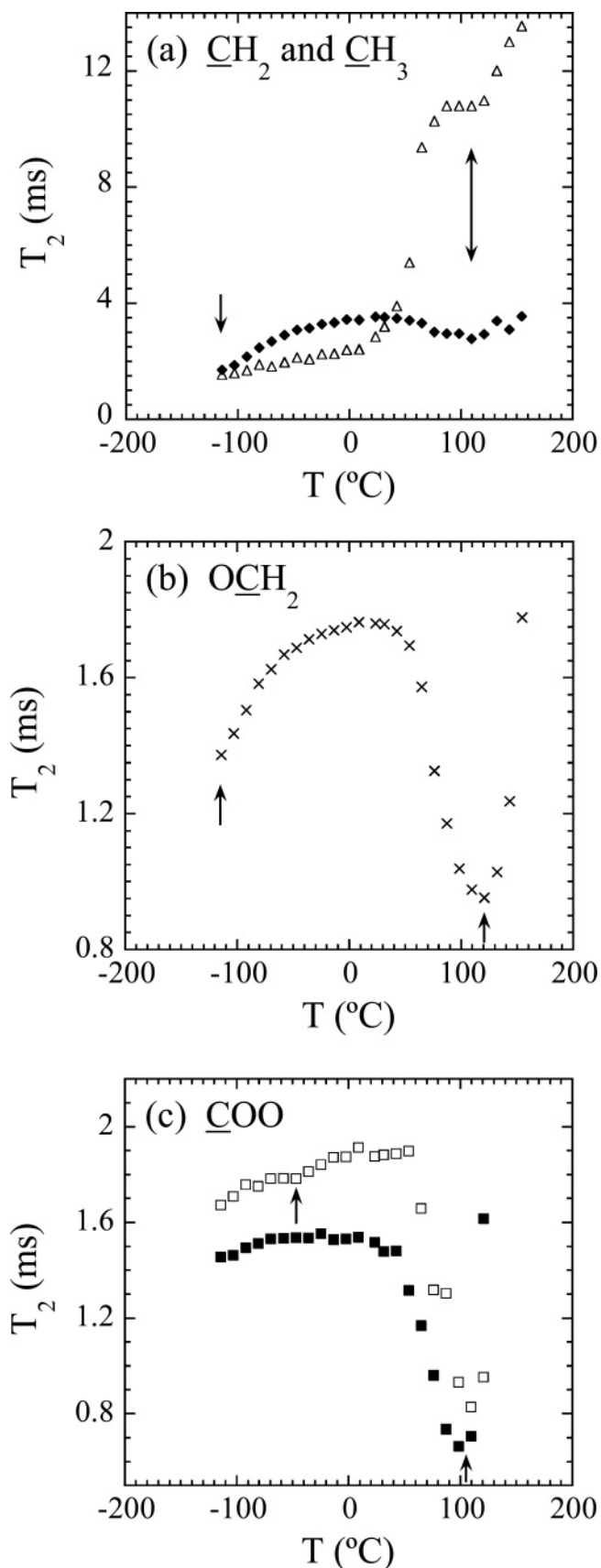


Figure 9. Transverse relaxation times, T_2 , of (a) the CH_3 (Δ) and CH_2 (\blacklozenge) carbons, (b) the OCH_2 carbon, and (c) the COO_a (\blacksquare) and COO_b (\square) carbonyl groups in poly(di-*n*-propylitaconate) as a function of temperature. Arrows indicate the position of the different T_2 minima.

sponds to a broadening of about 10 Hz that can be associated again to inhomogeneities of the static field. Because of this

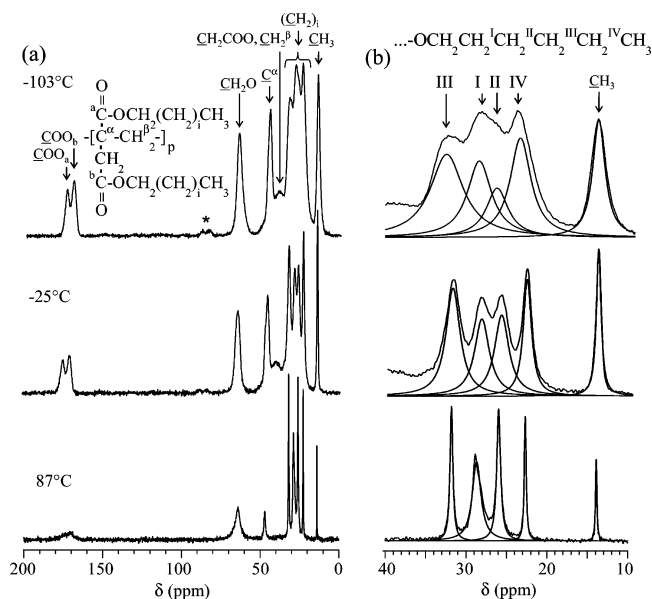


Figure 10. Experimental (a) and simulated (b) 75 MHz MAS/CP/DD ^{13}C NMR spectra of solid poly(di-*n*-hexylitaconate) at different temperatures. The spectral assignments are shown on the ^{13}C NMR spectra at -103 $^{\circ}\text{C}$ (the asterisks indicate the location of the spinning sidebands in (a)). Insets: (a) chemical formula of PDHI, (b) assignment of the side-chains methylene carbons in PDHI.

additional effect, T_2 variations resulting from molecular motions of the COO_b group are hidden below -50 $^{\circ}\text{C}$.

Concerning the main-chain carbons, a clear chemical shift variation with temperature toward lower field was observed for C^{α} , CH_2^{β} , and CH_2COO . In the investigated temperature range, the variation of the chemical shift is of the order of 3 ppm for C^{α} , with a 1 ppm variation in the temperature range from 48 to 76 $^{\circ}\text{C}$. The frequency of the motions observed in this region is of the order of 75 Hz. For CH_2^{β} and CH_2COO , a 5 ppm variation takes place between 54 and 87 $^{\circ}\text{C}$, indicative of molecular motions at frequencies of the order of 375 Hz. It must be noticed that the CH_2^{β} and CH_2COO chemical shifts share similar temperature dependence, suggesting that these two carbons are involved in correlated motions, as already observed in PDMI. The temperature dependence of $t_{1/2}$ for the two methylene units of the main chain is shown in Figure 7a. The $t_{1/2}$ values are equal to 17 μs within experimental error between room temperature and 121 $^{\circ}\text{C}$, which indicates that the CH_2^{β} and CH_2COO carbons do not undergo any local motions at a frequency equal to or higher than 10^5 Hz in this temperature range. Above 121 $^{\circ}\text{C}$, there is a clear reduction of the strength of the dipolar coupling, indicating the existence of motional processes of the main chains in the 10^5 Hz region. At 143 $^{\circ}\text{C}$, the values obtained for the $t_{1/2}/t_{1/2-\text{rigid}}$ ratio indicate the existence of correlated conformational jumps²⁸ within the main chain. It is also interesting to note that, at a given temperature, the $t_{1/2}$ values in PDPI and, therefore, the amplitude of the molecular motions, decrease from the end of the side chain to the main chain.

4.3. Poly(di-*n*-hexylitaconate). MAS/CP/DD ^{13}C NMR spectra of PDHI recorded at various temperatures are shown in Figure 10, together with the spectral assignments and the chemical formula of the polymer. The spectra exhibit two modifications on varying temperature: a variation of the width at mid-height for all the carbons in the repeat unit and a variation of the chemical shift of the quaternary carbon C^{α} .

At -110 $^{\circ}\text{C}$, the peaks associated with the alkyl side-chain carbons are so broadened that the resolution has completely disappeared (see Figure 10b). On the opposite, at 87 $^{\circ}\text{C}$, the

lines are narrow and well resolved. This important line-broadening for the aliphatic carbons in PDHI is a clear indication of the modulation of the dipolar interaction by molecular motions of the side chains. To determine $T_2 = (\pi\Delta\nu_{1/2})^{-1}$ for the $(\text{CH}_2)_i$ and CH_3 units, the composite line was decomposed into five Lorentzian functions centered around the chemical shifts determined at high temperature. This decomposition is shown in Figure 10b. There, it can be seen that the individual lines related to the methylene units are well-defined and the error bars for T_2 in the temperature range between 0 and 80 °C are of the order of 2%. The highest accuracy is obtained for the methyl groups, as the corresponding line is isolated on the full temperature range. The temperature dependences of T_2 for the individual side-chain methyl and methylene carbon lines are plotted in Figure 11a. They all exhibit a minimum at a temperature equal to or lower than -114 °C and a complex temperature behavior at higher temperatures, which suggests the existence of several motional modes. The clearest results are observed for the CH_3 carbon, which shows two minima around 20 and 55 °C that indicate molecular motions at frequencies of the order of 83 kHz. In the same way, the carbon line for the OCH_2 carbon shows broadenings that are dominated by the modulation of the dipolar coupling (Figure 11b). Two T_2 minima are observed: a first minimum in the vicinity of -114 °C and a second minimum with stronger amplitude at 65 °C. Although not well-defined, a third minimum can be seen around 31 °C. These minima are again associated to motions with frequencies of about 83 kHz.

Figure 11c shows the temperature dependences of T_2 for the individual lines obtained by decomposing the carbonyl line into two Lorentzian functions. They exhibit a single minimum located at 54 and 65 °C for COO_a and COO_b , respectively. The broadening observed from -80 to -114 °C is of the order of 10 Hz and can be associated to inhomogeneities of the static field.

Finally, the C^α chemical shift variation is of the order of 2 ppm toward the lower field in the temperature range investigated. A chemical shift variation of about 1 ppm is observed between 9 and 31 °C, which indicates conformational changes in the main-chain or adjacent side-chain bonds.

In PDMI, measurements of the dynamic order parameter associated with the carbonyl carbons (Figure 5) show that large-amplitude motions of the carbonyl groups require a significant reorientation of the local main-chain axis that can only occur in the vicinity of the glass transition. Figure 12 displays results obtained for $\langle P_2 \rangle$ in the three PDAI's investigated. For all the samples, the dynamic order parameter decreases as the temperature increases, i.e., as it goes toward an isotropic motion. However, close to and above T_g , $\langle P_2 \rangle$ still displays remarkably high values for both carbonyl carbons. In a similar way, Kulik et al.²³ reported unusually high values of $\langle P_2 \rangle$, at temperatures well above T_g , for the carbonyl carbon of poly(ethyl methacrylate) (PEMA). This result was explained in terms of an anisotropic motion of the PEMA chain and of a residual order above T_g due to extended chain conformations.²³ Such a residual conformational order was also observed with a smaller extension in PMMA.²³ If we use these conclusions to interpret data reported in Figure 12, we can conclude that the chain motions in PDAI's are anisotropic and that a substantial conformational order is present in the molten state. As previously observed,²³ this phenomenon depends on the side-chain length. Indeed, at a given distance from T_g , $\langle P_2 \rangle$ decreases from $n = 1$ to $n = 6$. This result emphasizes the importance of the side groups on the overall dynamics of PDAI's. Finally, note that, in a recent

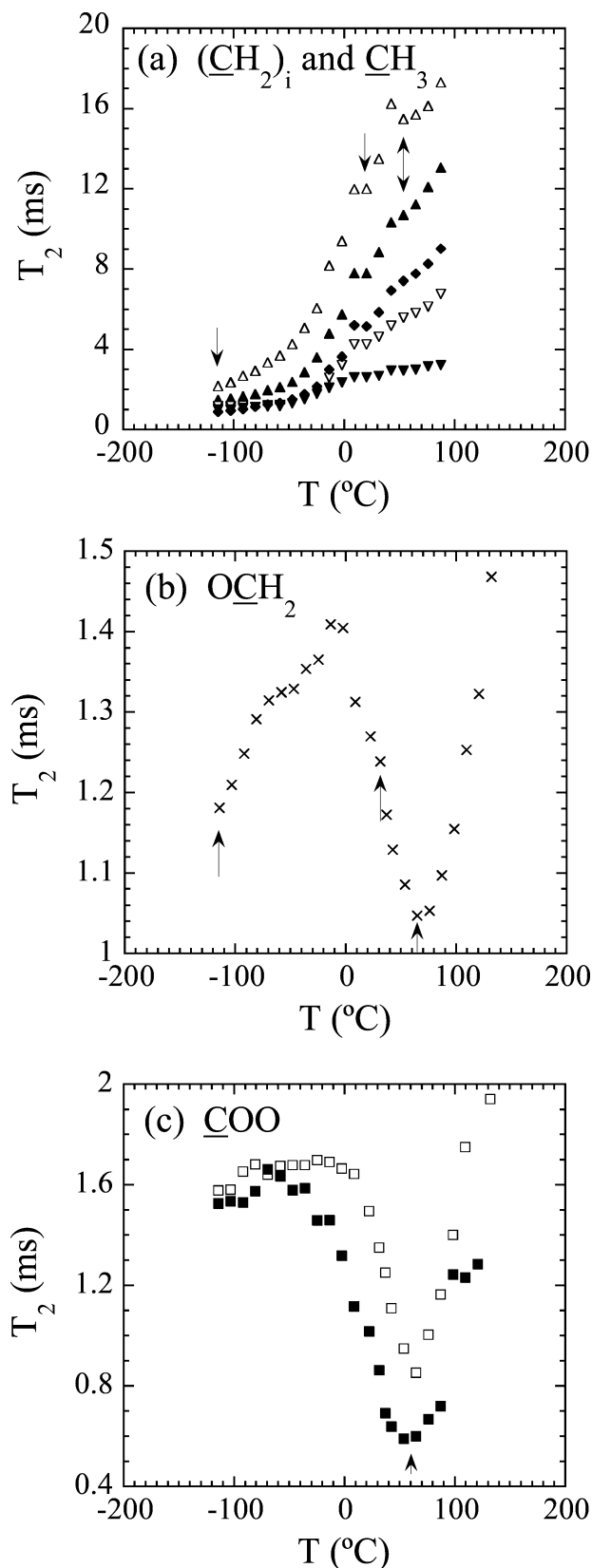


Figure 11. Transverse relaxation times, T_2 , of (a) the CH_3 (Δ), CH_2^{IV} (\blacktriangle), CH_2^{III} (\blacklozenge), CH_2^{II} (∇), CH_2^{I} (\blacktriangledown) carbons, (b) the OCH_2 carbon and (c) the COO_a (\blacksquare) and COO_b (\square) carbons in poly(di-*n*-hexylitaconate) as a function of temperature. Arrows indicate the position of the different T_2 minima.

NMR study, Wind et al.²⁹ showed that poly(*n*-alkyl methacrylate)s retain conformation memory, leading to an additional slowest process (*isotropization of the main chain*) as compared

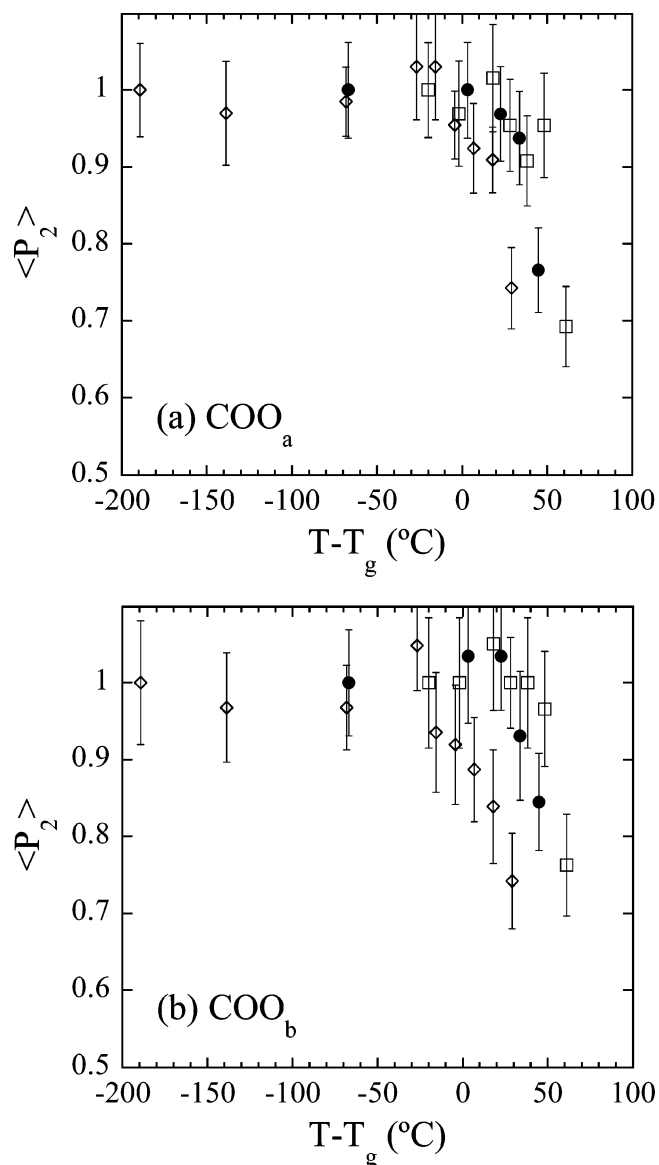


Figure 12. Evolution of the dynamic order parameter as a function of the $T - T_g$ temperature difference for COO_a (a) and COO_b (b) in PDMI (◇), PDPI (●), and PDHI (□).

to the usual $\alpha\beta$ relaxation reported so far. It is reasonable to think that the same behavior would occur in PDAI's.

5. Discussion

From the T_2 determinations for the different carbons of the PDAI samples, it is possible to derive the correlation times, τ_c , by using eqs 2 and 4 for protonated and unsaturated carbons, respectively. The prefactor in both equations was determined by using the relationship $\omega\tau_c = 1$ which applies at the T_2 minimum. Note that, because τ_c is calculated from the values of T_{2m} (or $T_{2\sigma}$), it is necessary to subtract the T_{2res} contribution that corresponds to the residual line width due to static effects. The T_{2res} contribution was obtained from the plateau value observed in the T_2 variations versus temperature. The frequencies $\nu = (2\pi\tau_c)^{-1}$ deduced from the various T_2 minima and τ_c calculations are plotted in Figure 13 for PDMI (a), PDPI (b), and PDHI (c). These relaxation maps include dielectric spectroscopy results from our previous study⁹ on these systems. They lead to the following identification of the moving units involved in the different relaxation processes initially characterized by dielectric spectroscopy:

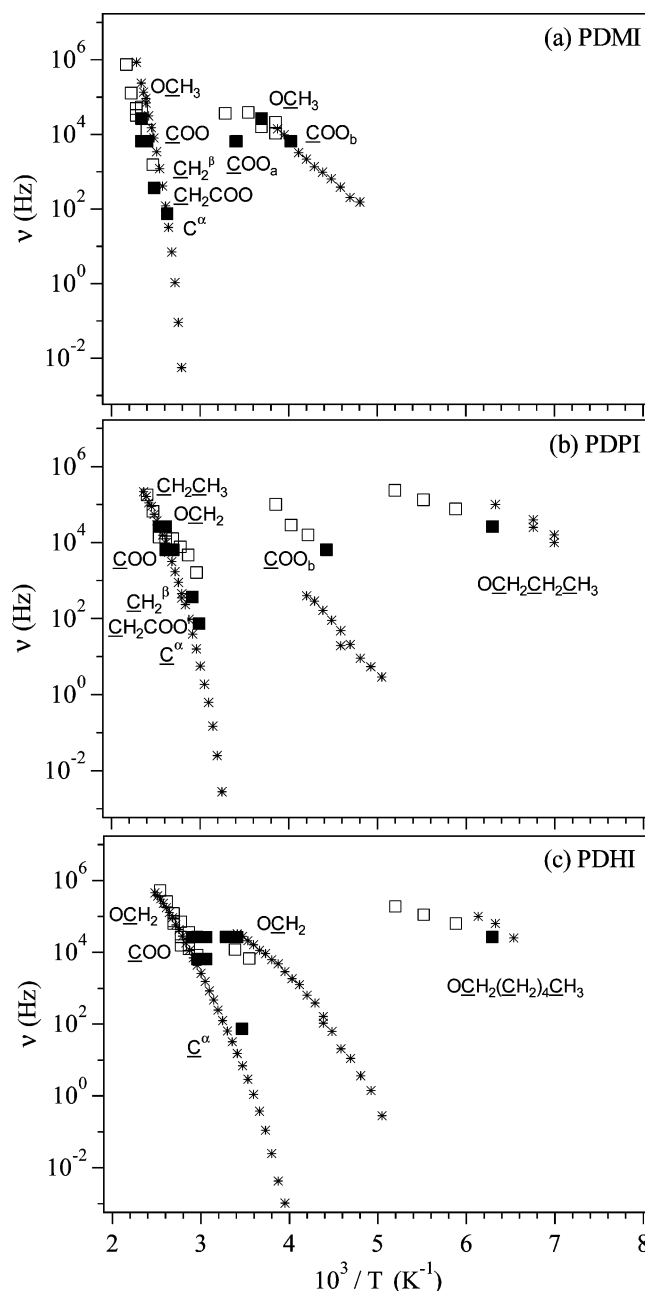


Figure 13. Relaxation map for PDMI (a), PDPI (b), and PDHI (c), including the NMR results obtained from T_2 minima (■) and calculated correlation times (□), and the dielectric data (*) from ref 9.

5.1. γ Relaxation. The γ relaxation was detected by using solid-state ¹³C NMR for PDAI's containing three carbon atoms at least in the side chains. From the comparison of NMR and dielectric data reported for PDPI (Figure 13b) and PDHI (Figure 13c), it can be concluded that the γ process is clearly due to motions of the alkyl units in the side chains and that its position does not depend of the side-chain length, in agreement with other authors.^{3,7,30} Here, we would like to emphasize that the position of the low- T minima, which we took at -114 °C for the alkyl units in PDPI and PDHI, is in qualitative agreement with the position of the dielectric data. Moreover, the slight discrepancy that we can observe in Figures 13b and c indicates that the NMR minima should occur at a slightly lower temperature than -114 °C, which could not be assessed experimentally. The molecular origin of the low-temperature relaxation was recently investigated for two poly(di-*n*-chloro-alkylitaconate)s by using molecular mechanics calculations.³¹

Results obtained by Sanchis et al.³¹ show that the γ relaxation is a localized noncooperative rotation around the central O—C—C—Cl or C—C—C—Cl sequence, with an energy barrier of 25.2 kJ·mol⁻¹ that can be compared to the apparent activation energy obtained for PDPI: $E_{\text{app}} = 16 \pm 5$ kJ·mol⁻¹ and 24 kJ·mol⁻¹ from the present NMR and previous dielectric spectroscopy results,⁹ respectively.

5.2. β_{fast} or α^{L} Relaxation. For the lower derivatives ($n = 1$ and $n = 3$), the dielectric spectroscopy results⁹ demonstrated the existence of a noncooperative process, called β_{fast} . This process was previously described by Diaz-Calleja et al.⁷ By comparing the β_{fast} relaxation in PDMI to the transitions observed in poly(methyl methacrylate) and poly(monomethyl itaconate), the authors attributed the β_{fast} relaxation in PDAI's to motions of the ester group separated from the main chain by a CH₂ unit. The correlation times determined selectively for the COO_b carbonyl group motion by using solid-state ¹³C NMR (see Figure 13a and b) strongly support this identification. The apparent activation energy deduced from NMR for PDMI is 38 ± 13 kJ·mol⁻¹, in good agreement with the value reported by Diaz-Calleja et al.⁷ $E_{\text{app}} = 41.5$ kJ·mol⁻¹, and with our dielectric spectroscopy data,⁹ $E_{\text{app}} = 41$ kJ·mol⁻¹. In the case of PDPI, the NMR data are slightly shifted toward higher temperature compared to the dielectric data. However, the apparent activation energies determined from NMR ($E_{\text{app}} = 38 \pm 5$ kJ·mol⁻¹) and from dielectric spectroscopy⁹ (50 kJ·mol⁻¹) are in good qualitative agreement.

Turning now to the higher derivative (PDHI), a relaxation process (α^{L}) with the typical features of a dynamic glass transition (non-Arrhenius behavior and cooperativity) was found by dielectric spectroscopy⁹ in the same temperature and frequency ranges as the previously discussed β_{fast} process. In Figure 13c, the NMR results clearly show the contribution of the alkyl side-chains units in the α^{L} relaxation, and we can note that this result is in agreement with a previous investigation on poly(di-*n*-octylitaconate).³² However, in ref 9, we demonstrated that the α^{L} relaxation in the derivatives with six carbon atoms at least in the side chains involves both the alkyl side chains and the COO_b groups. As a matter of fact, the NMR results do not show any contribution of the carbonyl group to this process (see Figure 13c). It is very likely that the amplitude of the motion of this group is too low to be detected by NMR. Indeed, it is reasonable to think that an increase of the side-chain length up to $n = 6$ may lead to a slowing down of the COO_b dynamics.

5.3. β_{slow} Relaxation. From the results reported in Figure 13a for PDMI, the β_{slow} relaxation can be assigned to motions of the carbonyl group directly bonded to the main chain, COO_a. In PDPI and PDHI, this process is not detected because, at such high frequencies ($\sim 10^4$ Hz), the β_{slow} relaxation and the α relaxation merge.⁹

5.4. α or α^{U} Relaxation. In the three samples, the NMR results nicely show that all the chemical units, and in particular the main-chain units, are involved in the segmental relaxation. The agreement of the correlation times with the dielectric data is excellent, and the NMR data reproduce very well the typical WLF behavior expected for the glass-transition phenomena.

Finally, it is interesting to consider the additional relaxation process observed in the higher poly(*n*-alkyl methacrylate)s at temperatures below the conventional glass-transition temperature. This process was initially reported by Beiner et al.^{33–36} as the α^{PE} process and associated with motions of the alkyl side chains. The α^{PE} relaxation exhibits some common features with the α^{L} relaxation in PDAI's, except that it does not exhibit a dielectric activity because no dipole reorientation is involved.

In a recent effort to corroborate the attribution of the α^{PE} process, Hiller et al.³⁷ determined the half-width at mid-height for the main-chain and side-chain CH₂ carbons of poly(*n*-decyl methacrylate) in MAS/CP/DD ¹³C NMR spectra. The temperatures of the maximum broadening were inserted in an Arrhenius plot, and the points associated to the main chain and the side chain, at the observation frequency of the NMR measurements, were found to match with the glass transition and the α^{PE} process, respectively. These results emphasize the close similarity that exists between the α^{PE} process observed in the higher poly(*n*-alkyl methacrylate)s and the α^{L} relaxation of PDAI's.

6. Conclusions

The present study of poly(di-*n*-alkylitaconate)s with various side-chain lengths illustrates the ability of high-resolution solid-state NMR to selectively identify the various motions that are involved in the mechanical and dielectric transitions of these polymers: only the spectral lines of carbons belonging to the moving part of the molecule are affected and permit a clear interpretation of the motions. The γ transition is clearly due to localized motions within the alkyl part of the side chains. The β_{fast} relaxation involves motions of the COO_b group separated from the main chain by a CH₂ unit, whereas the β_{slow} relaxation can be assigned to motions of the carbonyl group directly bonded to the main chain, COO_a. In PDAI's with long alkyl side groups, the present NMR results support the nanophase separation picture characterized by the existence of two coexisting glass transitions, α^{L} and α^{U} . The α^{L} relaxation appears to be associated with the cooperative motion of the whole alkyl side chains, together with the carboxyl group of the side chain next to the CH₂ spacer unit. The α^{U} relaxation corresponds to the onset of motions involving the main-chains units and is decoupled from the α^{L} process. The results discussed in this work are in good agreement with our previous dielectric relaxation study⁹ and give a deeper insight of the motional behavior of these polymers in the solid state.

Acknowledgment. We gratefully acknowledge Dr. V. Arrighi and Dr. P. F. Holmes (Department of Chemistry, Heriot-Watt University, Edinburgh, Scotland) for their kind gift of PDAI samples and helpful discussions.

References and Notes

- (1) Cowie, J. M. G.; McEwen, I. J.; Pedram, M. Y. *Macromolecules* **1983**, *16*, 1151.
- (2) Cowie, J. M. G.; Ferguson, R.; McEwen, I. J.; Pedram, M. Y. *Macromolecules* **1983**, *16*, 1155.
- (3) Cowie, J. M. G.; Henshall, S. A. E.; McEwen, I. J.; Velickovic, J. *Polymer* **1977**, *18*, 612.
- (4) Cowie, J. M. G.; Haq, Z.; McEwen, I. J. *J. Polym. Sci., Polym. Phys. Ed.* **1979**, *17*, 771.
- (5) Cowie, J. M. G. *Pure Appl. Chem.* **1979**, *51*, 2331.
- (6) Cowie, J. M. G.; Haq, Z.; McEwen, I. J.; Velickovic, J. *Polymer* **1981**, *22*, 327.
- (7) Diaz Calleja, R.; Gargallo, L.; Radic, D. *Macromolecules* **1995**, *28*, 6963.
- (8) Arrighi, V.; McEwen, I. J.; Holmes, P. F. *Macromolecules* **2004**, *37*, 6210.
- (9) Genix, A.-C.; Lauprêtre, F. *Macromolecules* **2005**, *38*, 2786.
- (10) Genix, A.-C.; Lauprêtre, F. Accepted in *J. Non-Cryst. Solids* **2006**, Proceedings of the Fifth International Discussion Meeting on Relaxations in Complex Systems, Lille, France, July 7–13, 2005.
- (11) Bielecki, A.; Burum, D. P. *J. Magn. Reson.* **1995**, *116*, 215.
- (12) Herzfeld, J.; Berger, A. E. *J. Chem. Phys.* **1980**, *73*, 6021.
- (13) Vanderhart, D. L.; Earl, W. L.; Garroway, A. N. *J. Magn. Reson.* **1981**, *44*, 361.
- (14) Rothwell, W. P.; Waugh, J. S. *J. Chem. Phys.* **1981**, *74*, 2721.
- (15) Suwelack, D.; Rothwell, W. P.; Waugh, J. S. *J. Chem. Phys.* **1980**, *73*, 2559.
- (16) Woessner, D. E. *J. Chem. Phys.* **1962**, *36*, 1.

- (17) Lauprêtre, F.; Monnerie, L.; Virlet, J. *Macromolecules* **1984**, *17*, 1397.
- (18) Horta, A.; Hernandez-Fuentes, I.; Gargallo, L.; Radic, D. *Makromol. Chem., Rapid Commun.* **1987**, *8*, 523.
- (19) Lopez-Carrasquero, F.; Martinez de Ilarduya, A.; Cardenas, M.; Carrillo, M.; Arnal, M. L.; Laredo, E.; Torres, C.; Mendez, B.; Müller, A. J. *Polymer* **2003**, *44*, 4969.
- (20) Mandelkern, L. *Pure Appl. Chem.* **1982**, *54*, 611.
- (21) Mehring, M. *High-Resolution NMR in Solids*; Springer-Verlag: New York, 1983.
- (22) Beaume, F.; Thesis, Université Paris VI, 1996.
- (23) Kulik, A. S.; Radloff, D.; Spiess, H. W. *Macromolecules* **1994**, *27*, 3111.
- (24) Bordes, B.; Thesis, Université Paris VI, 1999.
- (25) Abragam, A. *The Principles of Nuclear Magnetism*; Oxford University Press: London, 1961.
- (26) Tonelli, A. E. *NMR Spectroscopy and Polymer Microstructure*; VCH Publishers, Deerfield Beach, FL, 1989.
- (27) Born, R.; Spiess, H. W. *Ab Initio Calculations of Conformational Effects on ¹³C NMR Spectra of Amorphous Polymers*; Springer-Verlag: New York, 1997.
- (28) Oulyadi, H.; Thesis, Université Paris VI, 1989.
- (29) Wind, M.; Graf, R.; Heuer, A.; Spiess, H. W. *Phys. Rev. Lett.* **2003**, *91*, 155702.
- (30) Shimizu, K.; Yano, O.; Wada, Y. *J. Polym. Sci., Polym. Phys. Ed.* **1975**, *13*, 1959.
- (31) Sanchis, M. J.; Diaz Calleja, R.; Pelissou, O.; Gargallo, L.; Radic, D. *Polymer* **2004**, *45*, 1845.
- (32) Genix, A. C.; Lauprêtre, F. *Polym. Prepr. (Am. Chem. Soc., Div. Polym. Chem.)* **2003**, *44*, 305.
- (33) Beiner, M.; Schröter, K.; Hempel, E.; Reissig, S.; Donth, E. *Macromolecules* **1999**, *32*, 6278.
- (34) Beiner, M. *Macromol. Rapid Commun.* **2001**, *22*, 869.
- (35) Beiner, M.; Kabisch, O.; Reichl, S.; Huth, H. *J. Non-Cryst. Solids* **2002**, *307*, 658.
- (36) Beiner, M.; Huth, H. *Nature Mater.* **2003**, *2*, 595.
- (37) Hiller, S.; Pascui, O.; Kabisch, O.; Reichert, D.; Beiner, M. *New J. Phys.* **2004**, *6*, 1.

MA060730C